



AIAS 2018 International Conference on Stress Analysis

Fatigue Life Estimation of a Military Aircraft Structure subjected to Random Loads

G. Zucca^{a,*}, F. Cianetti^b, M. Palmieri^b, C. Braccisi^b, F. De Paolis^a

^aItalian Air Force, Flight Test Center, Technology Materials for Aeronautics and Space Department, Military Airport M. De Bernardi, via Pratica di Mare, 000040 Pomezia (RM), Italy.

^bUniversity of Perugia, Department of Engineering, via G. Duranti 93, 06125 Perugia, Italy.

Abstract

The suspension system of external stores of a military aircraft has reached the fatigue life limit estimated during the design phase, however, some elements suggest that the duration of the structure has been largely underestimated. This work aims to re-evaluate the fatigue life of the system and the potential extension of its use following an experimental numerical approach where, starting from a series of experimental flights in which the structure was instrumented, the forces acting on the system were calculated. Therefore, a methodology was developed to limit the damage calculation time using a hybrid approach that exploits the advantages deriving from the low computational burden typical of the methods in the frequency domain coupled with the Rainflow Counting precision. The study, although penalized by a series of conservative hypotheses, allowed to estimate a residual life equal to past life. It also provided important feedback on the field of application of advanced techniques for estimating the fatigue life of aeronautical structures subjected to random loading stories.

© 2018 The Authors. Published by Elsevier B.V.

This is an open access article under the CC BY-NC-ND license (<http://creativecommons.org/licenses/by-nc-nd/3.0/>)

Peer-review under responsibility of the Scientific Committee of AIAS 2018 International Conference on Stress Analysis.

Keywords: Damage; Fatigue; Frequency domain approach; Multiaxial stress state; Random loads; Finite Element Analysis.

1. Introduction

Estimation of the durability of structural components, seen from a procedural perspective, disregards the use and destination aspects, which are parts of machines, building constructions, biomechanical apparatuses, and substantially takes two forms: design and testing. Design, intended as an a priori evaluation of fatigue behavior, is placed in the advanced stages of the development of an object, while maintaining large margins of uncertainty: first of all the exercise. If in static or dynamic sizing it is possible to conservatively resort to the worst case, in durability it would be necessary to know in advance and punctually the history of the component to make a realistic evaluation. The life of the object is then estimated on the basis of hypothesis of use and often it is expressed in one or more corrective

* Corresponding author. Tel.: 0691292336.

E-mail address: guido.zucca@aeronautica.difesa.it

measures, generally aimed at reducing the stress intensification factors (eg connections), or the increase the material performances (shot peening, rolling, etc. ...) [Shigley et al. \(2002\)](#).

By virtue of what has been said, the component is then qualified and submitted to the durability test, this enters the testing field, i.e. the tests in which the operating conditions are replicated and the life simulated until the breakdown. The tests are often very long and expensive, the duration is the critical element and the acceleration of the tests, obtained by worsening the conditions of exercise, often leads to very conservative results [Niesłony et al. \(2016\)](#). The challenge undertaken by the research aimed at experimentation hinges on the concertation of the objectives of speed reliability and economic sustainability of the tests, which, as often happens in engineering, are difficult to reconcile. Once the project estimates have been verified, the component is then certified and based on the assessments above, the maintenance and/or controls are scheduled, identifying the critical areas, the appropriate techniques and the intervals. In a scenario where the designer is calculating the durability of a component based on an estimated exercise and the experimenter testing it on an accelerated qualification spectrum [Wang et al. \(2013\)](#), what happens when the component arrives at the end of his life without having given signs of failure? This is clearly attributable to the safety factors assumed in the design phase and mainly, as already mentioned above, to a use that has been overestimated for reasons of opportunity. The question we asked ourselves and was the harbinger of this work was therefore: is it possible, knowing the real history of use of an object, to estimate its residual life? The reasons for this question go beyond the mere academic interest and are to be found in the economic and logistical impact that the delayed or avoided replacement of a valuable component can have in a completely transversal context. This creates a figure that is halfway between the designer and the experimenter in which the skills of design, modeling and measurement are put in place in a multidisciplinary manner, with a view to improving and refining what is already existing. As a benchmark for the activity, the case deriving from a real need occurred on an external system of suspension of loads (e.g. fuel tanks) of a fleet of aircrafts operated by the Italian Air Force, developed and realized in the '70s, was used. The object of the study concerns the connection points between the aircraft and the system that had been built on the basis of a presumed operational use and whose duration in 4000 hours of operation was estimated. To date, after more than 25 years, the expiry of the useful life has come nearer, since the failure of the components has not been recorded, the residual life of the same has been estimated starting from a well-known and consolidated use history, developing the dissertation as follows.

In the first paragraph, for what is allowed by the secrecy constraints, the system will be described giving evidence of the: archive design documentation [NATO](#), schematization of the structure, idealization of the material and hypotheses at the base. In the second paragraph, the operational statistics and the guidelines used in the design of the experimental tests will be discussed, which will be given wide visibility of the management and results. The passage from the experimental data to the load spectra and then to the stress will be discussed in the third paragraph in which the fem model will be described and the results will be discussed. The fourth paragraph, dedicated to the estimation of durability, identifies all the critical aspects of the application of the classical theory to a real case, adopting an energetic model for the estimation of multiaxiality and proposing a hybrid method in which the analysis in the frequency domain [J. S. Bendat \(1964\)](#), [Pitoiset and Preumont \(2000\)](#), [Braccési et al. \(2015\)](#) is combined to Rainflow Counting in order to reduce calculation time. The time vs frequency comparisons will then be performed by correlating the results to the statistical indicators.

2. Historical Background

The possibility of suspending and transporting payloads outside an aircraft is a need felt since the dawn of the aeronautics, which even calls to mind the immediate application in the war, is widely used for the transport of various kind of pods (eg optical observation, radar) and fuel tanks [Gern and Librescu \(1998\)](#), [Lasek and Sibilski \(2002\)](#), [Chen et al. \(2002\)](#).

The aircraft object of the study, arrived in the second half of the operational life, is equipped with a multipurpose system of suspension of external payload constituted, for the part of interest, by two pylons located in the ventral part of the fuselage (Fig. 1), able to transport different types of payloads depending on the needs. The pylons are connected to the aircraft by means of two pins (Fig. 2) that represent the real object of the analysis, at the time of the design it was in fact estimated a nominal life of these objects in 4000 flight hours, from the analysis of the archive documentation we tried to reconstruct the steps followed by the designer to achieve this result. The estimate of durability was based

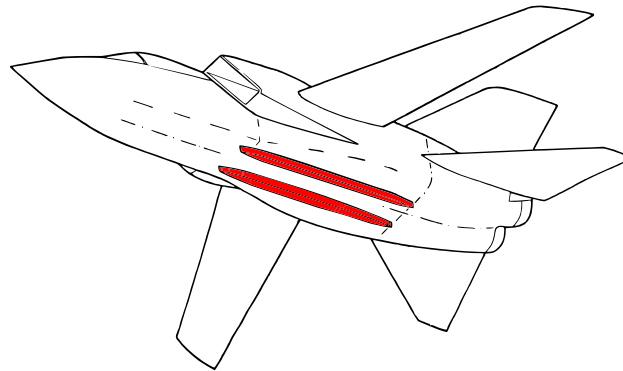


Fig. 1: Position of sub fuselage pylons.

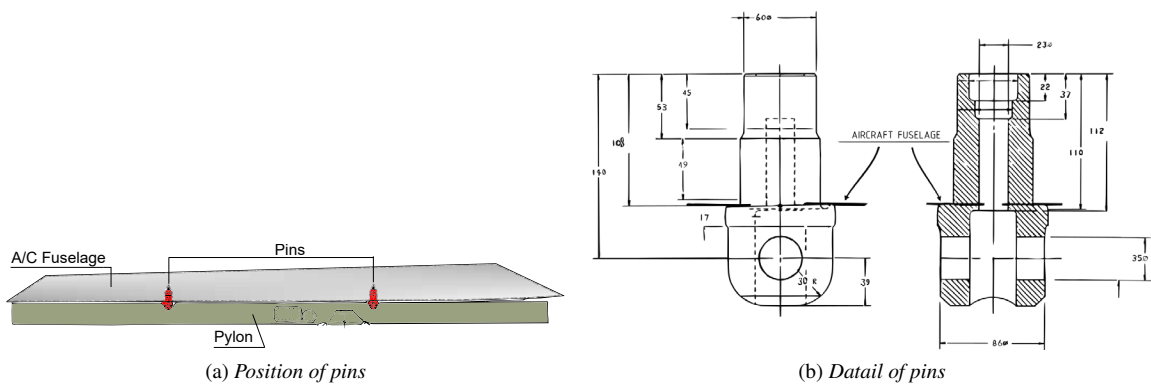


Fig. 2: Pins of connection.

on a usage requirement that led to identifying a series of maneuvers and quantifying the time spent by aircraft in each of them creating a "standard mission". The pylons had been instrumented with a set of accelerometers and by carrying out several flights in which the standard mission was carried out, each experimental maneuver had been characterized by obtaining the dynamic response of the system in terms of acceleration.

From the dynamic response through the reduction of masses and moments of inertia to the centers of gravity and the application of a simply supported scheme, the load spectra were inferred in terms of average and reversal load supported by the constraints of the structure subject to durability estimation. The critical sections of the constraints were then identified thus allowing the conversion from the force spectrum to stress spectrum. Following Palmgren-Miner's Miner (1945) rule every maneuver had been characterized in terms of damage and weighed according to its impact in the "standard mission". From the critical reading of the steps taken by the designers it was decided to use the same modus operandi, tracing the schematization of the pylon and deriving the information on the Wohler curve.

3. Standard Mission and Experimental Measures

From the statistical analysis of the operational life, flown by the fleet of aircraft, the actual life time spent on average by each aircraft in each representative maneuver has been extrapolated, so as to be able to summarize the history in a new mission "standard mission", this time defined ex post in spite of the estimates of the designers: the percentage values are shown in (Tab. 1). The pylon was then instrumented with a set of triaxial accelerometers oriented coherently with the reference system referred to the paragraph (4) and several flights of the standard mission were carried out as previously defined. The measurements, acquired with a sampling frequency of 4000 Hz, have variable duration

Table 1: Standard Mission Composition.

Id. number	Maneuver	Portion (%)
1	Take off & Taxi	22,25%
2	Low quote & Low speed stabilization	3,00%
3	Low quote & High speed stabilization	0,30%
4	Acceleration	0,05%
5	Turn	0,05%
6	High quote & Low speed stabilization	35,15%
7	High quote & High speed stabilization	35,15%
8	Landing	4,05%

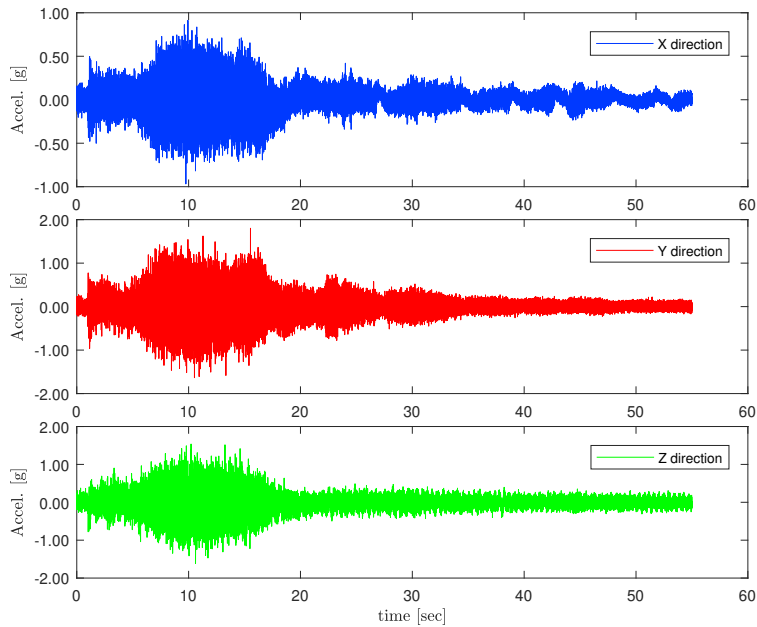


Fig. 3: Time Histories.

depending on the type of maneuver, in the case of events confined in time (ie: landing or take-off) it was decided to capture the phenomenon in its entirety, while in the case of cruises, a recording time of 60 seconds has been set.

3.1. Statistical analysis of the maneuvers

For each representative maneuver the acceleration time histories have been obtained (Fig. 3) and the statistic has been calculated (Fig. 4) that is the expected value, the standard deviation, the asymmetry index and the kurtosis index, defined respectively by formulations (1) Erto (2008).

$$m_X = \mathbb{E}(X) = \sum_{i=1}^{\infty} x_i p_i; \quad \sigma_X = \sqrt{\sum_{i=1}^{\infty} [x_i - \mathbb{E}(X)]^2 p_i}; \quad \gamma_X = \frac{\mathbb{E}[(X-m_X)^3]}{\sigma^3}; \quad \eta_X = \frac{\mathbb{E}[(X-m_X)^4]}{\sigma^4} \quad (1)$$

It is interesting to observe how in the maneuvers of a random nature (e.g. turns and stabilizations) the skewness and the kurtosis, of the amplitudes of the accelerations, tends towards zero and three respectively suggesting a Gaussian distribution.

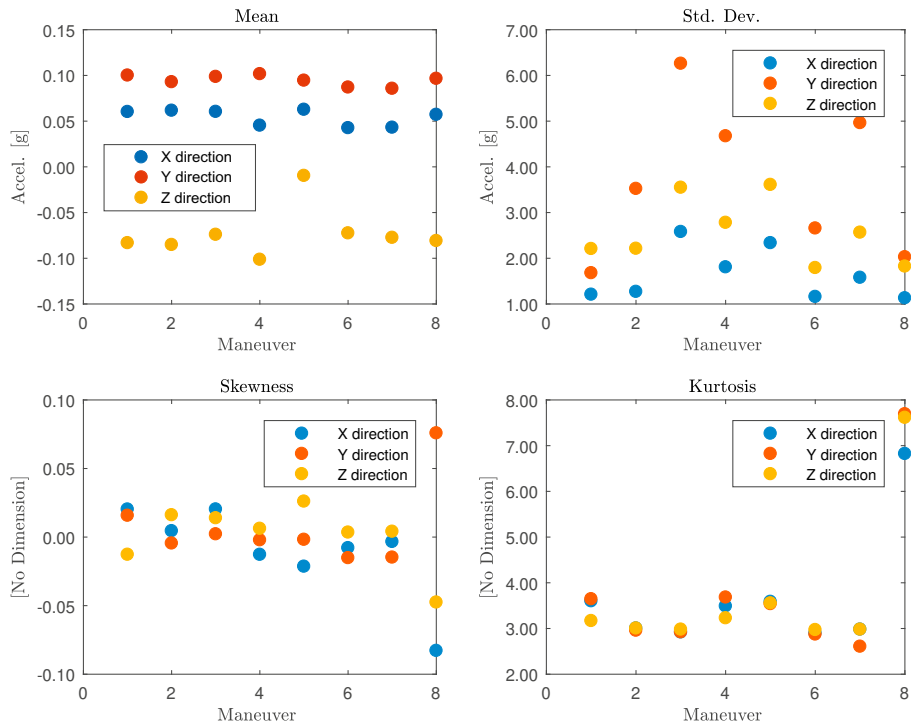


Fig. 4: Time Histories Statistic.

4. From acceleration to force to stress: the FEM model

The reference system that will be used in the continuation of the discussion coincides with the aircraft axes (Fig. 5 a)) where x represents the direction of advancement, z is directed towards the bottom and y oriented following the right hand rule.

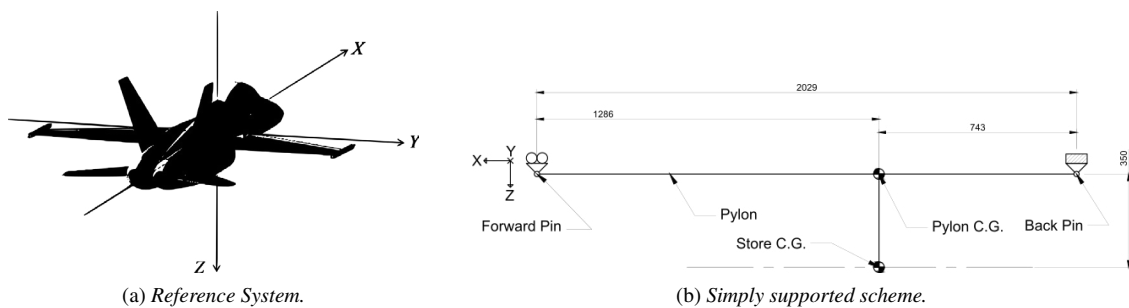


Fig. 5: Pylon idealization & reference system.

4.1. Schematization of the pylon

The coupling between the pins and the fuselage of the aircraft is made by a bolt, the connection with the pylon is of different nature: the rear in turn by means of a pin and a bush that allows to constrain the three degrees of translational freedom and the two rotational, allowing the rotation around the y axis, thus behaving like a hinge on the xz plane, the anterior by means of a pin and a slot which in addition also allows small long translations x thus

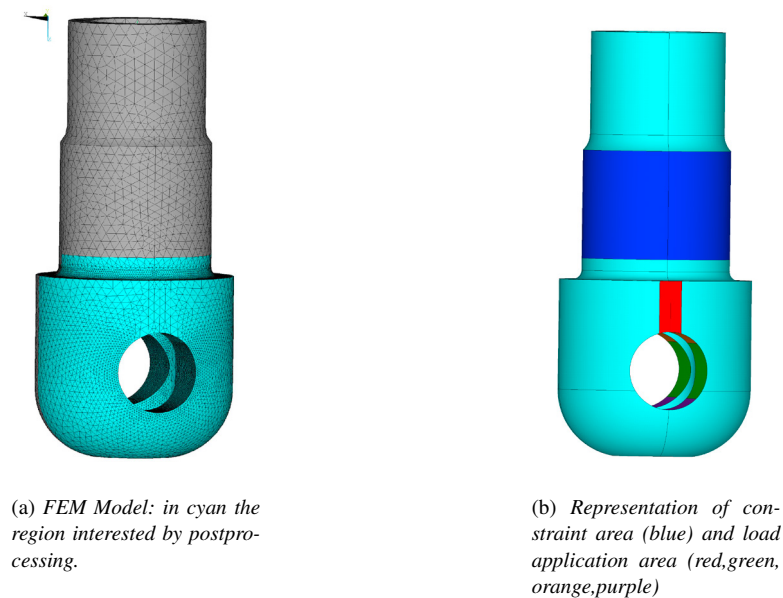


Fig. 6: FEM Model.

reducing to a trolley on the xz plane. The system can therefore easily be traced back to a simply supported scheme consisting of a beam constrained as in Fig. 5 b).

It was considered lawful for the study of the constraints only, in line with what was done in the past, to hypothesize the pilon-load assembly as a rigid system, i.e. as an accelerating oscillating body, whereby the masses and centers of gravity are known: from theory of constructions it is therefore possible to deduce the constraint reaction forces. Transforming the three acceleration time histories into nine strength stories, with zero moments around the y axis and zero x -direction reaction on the front pin.

4.2. The FEM model

From the force time history acting on the constraints it has been calculated the stress state realizing a finite element model in the ANSYS APDL environment, using the expedient of coating the solid with a thin skin of shell elements having infinitesimal thickness (order of 10^{-4} m) then structurally irrelevant (Fig. 6(a)). This technique, which goes well with the reasonable hypothesis in which the critical stress state for fatigue occurs on the outside of the component, is adopted with the dual purpose of obtaining a perfectly biaxial state of stress on the surface of the solid and reducing the computational burden of post processing to the skin elements only.

The FEM model is described in Fig. 6 were: on the left left a) the model is represented with cyan highlights the area where the skin elements were generated and then submitted to post processing. On the right b) the constrained zones (in blue) are highlighted, where it was applied, on the external nodes, a displacement constraints such as to replicate the constraint conditions represented in Fig. 5. In red, green, orange and purple are indicated the areas of application of the ideal loads, made by pressure loading, always with unitary result. The nine load conditions at the beginning of the paragraph were simulated with unitary force values, therefore, for each element, the nine stress tensors were linearly combined for the nine force time history, obtaining the pin stress history .

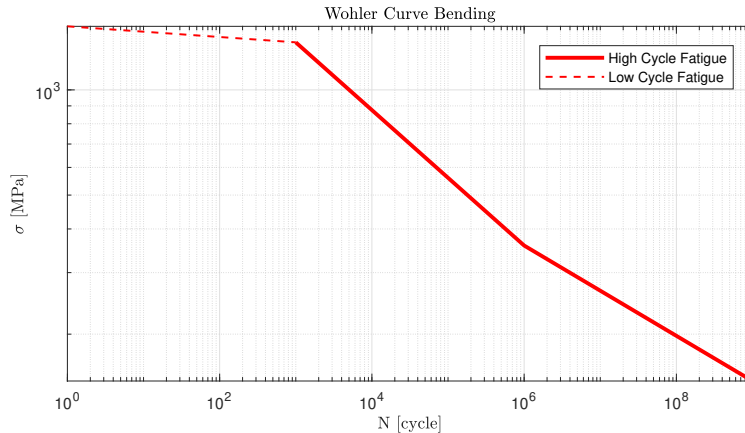


Fig. 7: Wohler Curve.

4.3. Wohler's curve

Also for the Wohler curve reference has been made to the archive documentation, the report is explained as follows:

$$\sigma = \alpha N^\beta \quad (2)$$

Where σ is the stress in MPa and N the number of cycles, the aforementioned curve assumes the trend of (Fig. 7), in

Table 2: Coefficients of the curve of Wohler.

α (MPa)	β	applicability
5287	-0,1938	$\forall N \in [10^3, 10^6]$
2137	-0,1292	$\forall N \in [10^6, \infty]$

which are to be considered at 50% reliability.

5. From stress to damage: multiaxiality and calculation times

A critical element in the evaluation of the durability of a component concerns the multiaxiality of stresses or how to establish a criterion that returns, given the temporal history of the stress tensor, a value comparable to the Wohler curve.

Given the type of material and the strength of the group's experience and work, it was decided to use the following procedure:

1. approach multiaxiality according to the formulation proposed by [Braccesi et al. \(2008\)](#), which suggests the calculation of the equivalent stress of Von Mises [Mises \(1928\)](#) starting from the construction of a new coherent stress tensor [Schijve and Yarema \(2003\)](#) as a function of frequency.

$$\sigma_{eqv} = trace([R] \cdot [G] \cdot [R]^T) \quad (3)$$

where R and G are defined in the works respectively [Braccesi et al. \(2018\)](#) and [Braccesi et al. \(2017\)](#). The tensor thus obtained is converted again to the time domain, by inverse Fourier transform, to obtain the equivalent stress time history;

2. count the cycles, of the equivalent stress time history thus obtained, using Rainflow Counting (RFC), taking into account the residues according to the formulation proposed by Clormann and Seeger, obtaining the load spectrum in terms of average and reversal stresses [Amzallag et al. \(1994\)](#);
3. apply Goodman’s theory to correct, on the High diagram, the alternating stress spectrum as a function of the average stress [Ekberg \(2002\)](#);
4. calculate the damage with the Palmgren Miner rule [Miner \(1945\)](#).

The calculation time required to perform the steps described therein, using an algorithm in the MatLab environment, on a good performance computer (Intel Xeon E3 1535 @ 3.10 GHz CPU, 32GB RAM, 1TB SSD), considering a model reduced to 30k elements and the number of time histories of 240000 samples, stood at 4305360 seconds: or about a month and a half to count the eight maneuvers, losing elasticity and readiness in varying the different parameters of the simulation (condensation of the model in critical areas, modification of the reliability of the Wohler curve, etc ...). It therefore seemed obligatory to circumscribe the solution of the model in the neighborhood of the areas most stressed by the specific load condition: in general a criterion was needed to define the a priori critical areas limiting to a reduced set of elements the calculation of the damage.

5.1. The Frequency Domain approach as a filter

It was therefore thought to move from the time domain to the frequency, going to synthesize the PSDs of the individual load stories and obtaining the stress tensor PSD (Fig. 8), for each element, such as:

$$[PSD_{\sigma}] = [\phi_{\sigma}]' [PSD_f] [\phi_{\sigma}] \tag{4}$$

Where:

- PSD_{σ} is the spectral power density of a biaxial random stress process (3 x 3 matrix);
- PSD_f is the spectral power density synthesized by the force time history (matrix 9 x 9);
- ϕ_{σ} is the stress tensor of the generic element for each load condition (9x3).

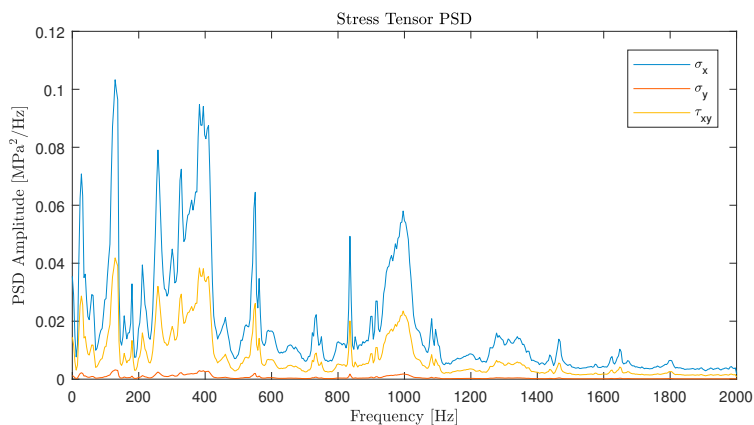


Fig. 8: Stress Tensor PSD.

From the stress PSDs an equivalent spectrum was then obtained by tracing the steps described by [Preumont \(2013\)](#), which extends the principle of the equivalent stress of Von Mises to the frequency domain, introducing the Von Mises equivalent stress PSD as:

$$[PSD_{eqv}] = trace[Q \cdot PSD_{\sigma}] = \sum_{i,j} Q_{i,j} \cdot PSD_{\sigma_{i,j}} \quad (5)$$

where

$$Q = \begin{bmatrix} 1 & -\frac{1}{2} & 0 \\ -\frac{1}{2} & 1 & 0 \\ 0 & 0 & 3 \end{bmatrix} \quad (6)$$

The result obtained was compared on the generic element with the stress PSD obtained by synthesizing the temporal process according to the [Braccesi et al.](#) formulation (step 1 of the procedure described here) obtaining the same result index of the coherence of the two approaches ([Fig. 9](#)).

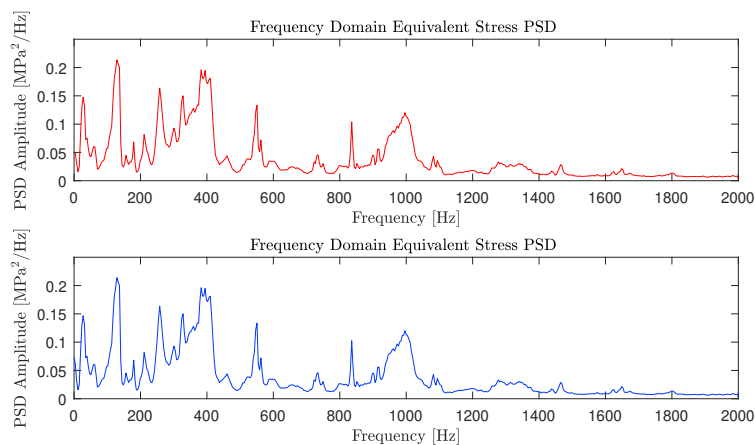


Fig. 9: Equivalent Stress PSDs.

The number of cycles was calculated from the equivalent stress PSD, by applying the relationship due to Rice:

$$n_0^+ = \frac{1}{2\pi} \left(\frac{m_2}{m_0} \right)^{\frac{1}{2}} \quad (7)$$

where

$$m_n = \int_0^{\infty} PSD_{eqv} \cdot f^n df \quad (8)$$

is defined as spectral moment of n-th order.

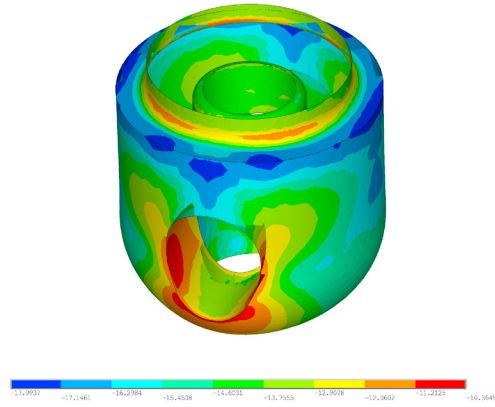


Fig. 10: Damage for Take-Off maneuver.

Rice’s formula shows how the relationship between the second order spectral moment and the PSD area is proportional to the number of zero up-crossing and therefore can be associated with the number of cycles in the unit of time for a zero mean Gaussian process. Finally, excluding that the stress process could be confined in a limited range of frequencies, and seeing the spectral power density of Fig. 9, an albeit vague, bimodal aspect, it was decided to apply the model proposed by Dirlik [Dirlik \(1985\)](#) in the calculation of the distribution of the amplitudes of the cycles. Under the Palmgren Miner hypothesis [Miner \(1945\)](#) the damage on all elements of the component is calculated, for each maneuver, in 35.7 seconds (Fig. 10).

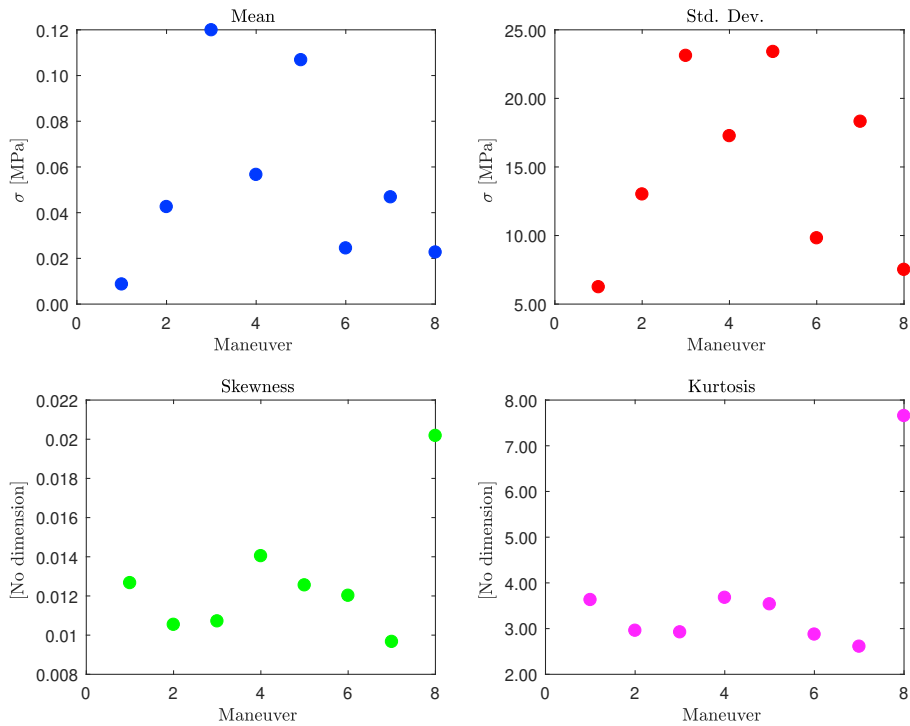


Fig. 11: Equivalent Stress Statistic.

5.2. Rainflow Counting & Durability

Once the 10^3 most damaged elements were identified for each maneuver was applied the procedure for calculating the damage over time, described at the beginning of par. 5, to a selection, no longer the result of an a priori choice, but which from time to time took into account the different damaging stresses. In this condition, the calculation times per maneuver were reduced to 17939 seconds: just under 5 hours.

For the set of significant elements identified, the equivalent stress history and than the statistics in Fig. 11 was calculated: the graphs show, as in the case of the accelerations (par. 3), the indicators of asymmetry and kurtosis tend to values typical of Gaussian distribution in stabilization and turning maneuvers, to detach completely in case of impulsive events such as landings. Furthermore, it should be noted that the trend of the standard deviation, which also represents the effective value of the stress process, can already be identified as the maneuvers with the highest damaging content (3 and 5). For each maneuver, referring to the most damaged element, we obtained the pdf of the

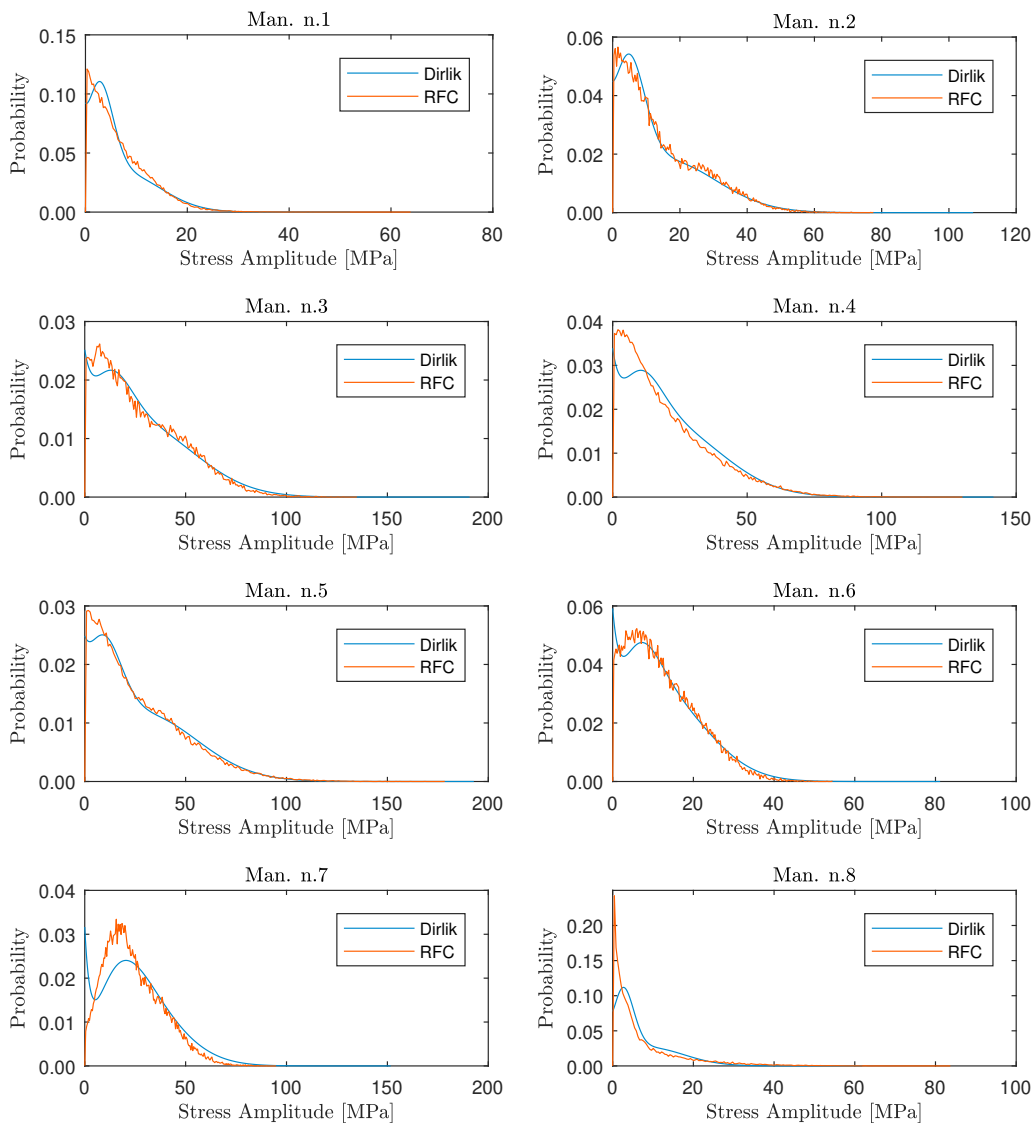


Fig. 12: Cycle Amplitude PDF: RFC vs Dirlik.

distributions of the cycles deriving from the RFC and compared with those previously obtained by the frequency approach (Fig. 12). As it was to be expected the less overlapped process concerns the landing maneuvers in which the high value of kurtosis bring a concentration of occurrences around the mean of the distribution of the stress process by shifting the barycentre of the pdf of the amplitudes towards the small values. Finally, we compared the damage value, obtained with the two techniques, on the reduced set of elements, obtaining the graphs of Fig. 13 (the damage is to be understood per unit of time). The graphs, in which the elements are ordered from the most to the least damaged in

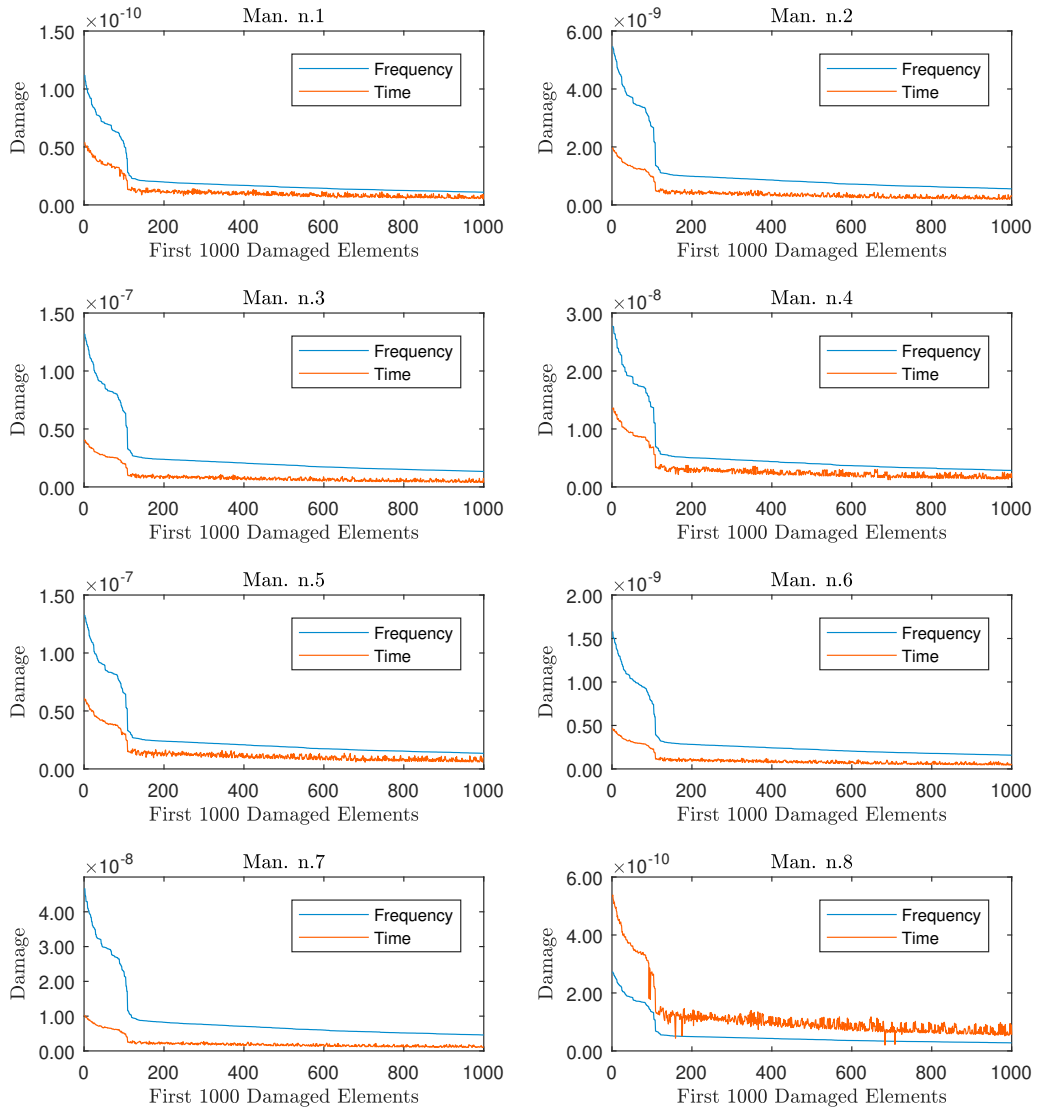


Fig. 13: Damage: RFC vs Frequency Domain Method.

abscissa, present an initial hump that represents the critical area for durability, and then settle at a value that could be defined as nominal: the evidence that the two zones coincide in all the maneuvers demonstrates the robustness of the implemented method and the validity of the frequency domain approach as estimator of the damage even in cases that it might seem not applicable.

In general, the frequency method overestimates the damage but preserving the same trend of the RFC approach, consistently with what previously observed the only critical condition in which the trend is reversed is in the landing maneuver.

Finally, the damage thus obtained and weighed according to the utilization estimates of Tab. 1 has led to estimate the useful life of the component in 8000 total flight hours or a remaining duration equal to how much has flown.

6. Conclusions

This work, articulating itself on the line of demarcation between design and testing, intends to conciliate the modern knowledge concerning the estimation of durability with the limits of the current computational powers, in a procedure where the frequency domain approach operates by reducing the size of the computational burden. In this way a meeting point is created between the needs of the certifier of robustness and certainty of calculation, typical of a time domain approach, and the ambition of the researcher to the use and investigation of increasingly efficient methods in the field of random fatigue.

From the calculations carried out, through the procedure developed, a duration of the double component was estimated compared to the forecasts made in the '70s, admitting the same safety margins. This is largely due to a real use of the aircraft far less severe as regards the suspension system of loads.

References

- Amzallag, C., Gerey, J.P., Robert, J.L., Bahuaud, J., 1994. Standardization of the rainflow counting method for fatigue analysis. *International Journal of Fatigue* doi:10.1016/0142-1123(94)90343-3, arXiv:arXiv:1011.1669v3.
- Braccesi, C., Cianetti, F., Lori, G., Pioli, D., 2008. An equivalent uniaxial stress process for fatigue life estimation of mechanical components under multiaxial stress conditions. *International Journal of Fatigue* doi:10.1016/j.ijfatigue.2007.09.011.
- Braccesi, C., Cianetti, F., Lori, G., Pioli, D., 2015. Random multiaxial fatigue: A comparative analysis among selected frequency and time domain fatigue evaluation methods. *International Journal of Fatigue* doi:10.1016/j.ijfatigue.2015.01.003.
- Braccesi, C., Morettini, G., Cianetti, F., Palmieri, M., 2017. Valutazione del Danneggiamento a Fatica effettuata mediante un Criterio Energetico di semplice Implementazione. . 6–9.
- Braccesi, C., Morettini, G., Cianetti, F., Palmieri, M., 2018. Development of a new simple energy method for life prediction in multiaxial fatigue. *International Journal of Fatigue* doi:10.1016/j.ijfatigue.2018.03.003.
- Chen, P.C., Sulaeman, E., Liu, D., Denegri, C., 2002. Influence of External Store Aerodynamics on Flutter/LCO of a Fighter Aircraft, in: 43rd AIAA/ASME/ASCE/AHS/ASC Structures, Structural Dynamics, and Materials Conference. doi:10.2514/6.2002-1410.
- Dirlik, T., 1985. Application of Computers in Fatigue Analysis , 234URL: <http://webcat.warwick.ac.uk/record=b1445503{-}S9>.
- Ekberg, A., 2002. Multiaxial Fatigue, in: Failure Fracture Fatigue. doi:10.1007/978-88-470-2336-9.
- Erto, P., 2008. Probabilità e Statistica per le scienze e l'ingegneria. third edit ed., McGraw-Hill.
- Gern, F.H., Librescu, L., 1998. Effects of externally mounted stores on aeroelasticity of advanced swept cantilevered aircraft wings. *Aerospace Science and Technology* doi:10.1016/S1270-9638(98)80008-4.
- J. S. Bendat, 1964. Probability functions for random responses. NASA report on contract NAS-4590 .
- Lasek, M., Sibilski, K., 2002. Modelling of external store separation. 40th AIAA Aerospace Sciences Meeting and Exhibit doi:10.2514/6.2002-687.
- Miner, M.A., 1945. Cumulative damage in fatigue. *American Society of Mechanical Engineers - Journal of Applied Mechanics* doi:10.1007/978-3-642-99854-6_35.
- Mises, R.V., 1928. Mechanik der plastischen Formänderung von Kristallen. *ZAMM - Journal of Applied Mathematics and Mechanics / Zeitschrift für Angewandte Mathematik und Mechanik* doi:10.1002/zamm.19280080302.
- NATO, . NATO Technical Report (Omissis...). Technical Report.
- Niesłony, A., Dziura, A., Owsiniński, R., 2016. Durability tests acceleration performed on machine components using electromagnetic shakers, in: Springer Proceedings in Mathematics and Statistics. doi:10.1007/978-3-319-42408-8_23.
- Pitoiset, X., Preumont, A., 2000. Spectral methods for multiaxial random fatigue analysis of metallic structures. *International Journal of Fatigue* doi:10.1016/S0142-1123(00)00038-4.
- Preumont, A., 2013. Twelve lectures on structural dynamics. *Solid Mechanics and its Applications* doi:10.1007/978-94-007-6383-8_1.
- Schijve, J., Yarema, S.Y., 2003. Fatigue of structures and materials in the 20th century and the state of the art. doi:10.1023/B:MASC.0000010738.91907.a9, arXiv:arXiv:1011.1669v3.
- Shigley, J.E., Mischke, C.R., Budynas, R.G., 2002. Shigley's Mechanical Engineering Design - 9th Ed. doi:10.1007/s13398-014-0173-7.2, arXiv:9809069v1.
- Wang, L., Burger, R., Lee, Y.L., Li, K., 2013. Random Vibration Testing Development for Engine Mounted Products Considering Customer Usage. *SAE International Journal of Materials and Manufacturing* doi:10.4271/2013-01-1007.